

Negative dispersion mirrors for dispersion control in femtosecond lasers: chirped dielectric mirrors and multi-cavity Gires–Tournois interferometers

R. Szipöcs^{1,2,*}, A. Köhási-Kis³, S. Lakó², P. Apai², A.P. Kovács⁴, G. DeBell⁵, L. Mott⁵, A.W. Louderback⁵, A.V. Tikhonravov⁶, M.K. Trubetskov⁶

¹R&D Lézer-Optika Bt, P.O. Box 622, 1539 Budapest, Hungary

²Research Institute for Solid State Physics and Optics, P.O. Box 49, 1525 Budapest, Hungary

³R&D Ultrafast Lasers Ltd, Konkoly Thege ut 29-33, 1121 Budapest, Hungary

⁴Dept. of Optics and Quantum Electronics, JATE University, Dóm tér 9, 6720 Szeged, Hungary

⁵MLD Technologies, 2672 Bayshore Parkway, Mountain View, CA 94043, USA

⁶Research Computing Center, Moscow State University, Moscow, 119899, Russia

Received: 1 October 1999/Revised version: 15 February 2000/Published online: 24 May 2000 – © Springer-Verlag 2000

Abstract. Chirped dielectric laser mirrors have been known for years as useful devices for broadband feedback and dispersion control in femtosecond pulse lasers. First we present a novel design technique referred to as frequency domain synthesis of chirped mirrors. These mirrors exhibit high reflectivity and nearly constant group delay over 150 THz supporting generation of sub-5-fs pulses in the visible. Afterwards, multi-cavity thin-film Gires–Tournois interferometers are introduced for the first time as an alternative approach to realize “negative dispersion mirrors”. These novel dielectric high reflectors exhibit reflectivities $R > 99.97\%$ and a negative group delay dispersion of $-50 \pm 1 \text{ fs}^2$ over a bandwidth of 56 THz. Dispersive properties originate from coupled resonances in multiple $\lambda/2$ cavities embedded in the layer structure. The general structure and performance of multi-cavity Gires–Tournois interferometers are compared to that of chirped dielectric mirrors and their distinct applications are discussed.

PACS: 42.15.Eq; 42.25.Bs; 42.40.Pa; 42.60.Da; 42.65.k; 42.79.Bh; 42.90.V

Recent development of ultrabroadband chirped dielectric laser mirrors (UBCMs) [1, 2] with prescribed phase properties brought revolutionary progress to the generation of femtosecond pulses both in the near infrared [3] and in the visible [4] spectral regimes. This resulted in optical pulses as short as 4.5 fs and 4.7 fs, respectively. With the combination of chirped mirror (CM) technology with air-silica microstructure optical fibers [5], further revolutionary progress in the generation and application of optical pulses of few cycles can be predicted: using standard sub-100-fs laser oscillators (for example, Ti:sapphire) with 1–2 nJ pulse energies, microstructure optical fibers for efficient continuum generation

and ultrabroadband chirped mirrors [1, 2] for dispersion management, sub-5-fs pulses could become an everyday tool in ultrafast laser laboratories.

In this paper we present our recent advances in fs laser technology that might help the ultrafast optics community to establish such ideal conditions. First we present a novel technique, *spatial frequency domain optimization* for designing discrete layer ultrabroadband chirped dielectric mirrors with prescribed second-, third-, and fourth-order dispersion. Since we perform our optimization process for few parameters (6–8) for full description of the chirped layer structure instead of using the individual layer thicknesses (40–60 parameters), we obtain an optimum solution within 1–2 min on a 266 MHz Pentium computer. The mirrors exhibit high reflectivity and nearly constant group delay dispersion over 210 THz and 140 THz, respectively, supporting sub-5-fs pulse generation in the visible spectrum [4, 6]. Second, an alternative approach for realizing “negative dispersion mirrors” with pure quadratic phase shift on reflection is introduced. We refer to them as *multi-cavity thin-film Gires–Tournois interferometers* (MCGTI): their dispersive properties originate from coupled resonances in multiple $\lambda/2$ cavities embedded in the layer structure. These novel devices exhibit extremely low reflection losses – when they are manufactured by our state-of-the-art ion-beam sputtering technique – ($R > 99.95\%$) and high-order dispersion-free group delay vs. frequency functions (for example, $-50 \pm 1 \text{ fs}^2$) over a bandwidth of 56 THz. Accordingly, they support clear, pedestal free sub-15-fs pulses, or sub-100-fs pulses tunable over a 100..120 nm around 800 nm in mirror-dispersion-controlled solid-state laser oscillators. Finally, we report on our recent *experimental results with the low loss, ion-beam-sputtered MCGTI-s* developed for mode-locked Ti:sapphire lasers [8].

1 Phase properties of dielectric mirrors

Optical thin-film devices play an important role in the final performance of fs laser systems: high reflectors (HR), output couplers (OC), antireflection (AR) coatings, or thin-film

*Corresponding author.

(Fax: +36-1/375-4553, E-mail: szipoecs@sunserv.kfki.hu)

spectral filters must be carefully designed or selected for the application problem [9]. They are based on the interference phenomenon of light and their theoretical analysis generally relies on the well-known matrix formalism [10, 11] derived from the Maxwell equations. The optical properties of optical interference coating are fully described by their wavelength- (or frequency)-dependent complex amplitude reflectance $r(\lambda)$ and transmittance $t(\lambda)$ functions. We recall that the amplitude reflectance is defined as the complex ratio of the reflected and the incident electric fields at the air/coating interface of the multilayer coating (see Fig. 1):

$$\bar{r}(\omega) = \frac{E_r(\omega)}{E_i(\omega)}. \quad (1)$$

Upon transmission through a spectral filter, optical pulses could become orders of magnitudes longer than the initial pulse due to spectral narrowing and/or dispersion [9], but in special cases such as optical tunnelling [12], considerable spectral broadening and pulse shortening could be observed [12]. The same effect can be easily observed, however, in ultrabroadband laser oscillators utilizing chirped mirrors for intracavity dispersion control [13, 14], in which the bandwidth of the intracavity spectrum is comparable to that of the output coupler [15].

In the case of dielectric high reflectors, the (intensity) reflectance, which is calculated as $R(\omega) = |r(\omega)|^2$, can be usually considered $R(\omega) \cong 1$, hence the frequency-dependent phase shift on reflection $\varphi(\omega) = -\arg(\bar{r}(\omega))$ determines the shape of a fs pulse after reflection on a dielectric multilayer mirror. Group delay, group-delay dispersion (GDD), third-order dispersion (TOD), and fourth-order dispersion (FOD) are calculated as the first, second, third, and fourth derivative of phase shift $\varphi(\omega)$ respectively by the angular frequency ω . Recently, phase properties of dielectric multilayers were discussed by Tikhonravov et al. from the aspect of mathematical complex analysis [16]. In the following, we briefly summarize the main *physical effects responsible* for the frequency-dependent group-delay on the reflection function, i.e. *dispersion of multilayer dielectric mirrors*.

The first effect, the *frequency-dependent penetration depth*, can be easily studied on the most widely used dielectric high reflector, the quarterwave ($\lambda/4$) stack, the operation of which is depicted in Fig. 2. A quarterwave stack consists of alternating high (H) and low (L) index layers of $\lambda/4$ optical thicknesses. As a result, a quarterwave mirror exhibits the highest reflectivity at the tuning (or reference) wavelength λ , at which wavelength the partial reflections on the high/low index interfaces meet exactly in phase, as shown in Fig. 2. The reflectivity of the $\lambda/4$ stack gradually decreases with increased detuning from the reference wavelength, in

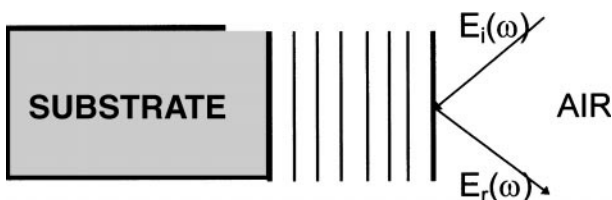


Fig. 1. Definition of the complex amplitude reflectance in the case of dielectric multilayer coatings

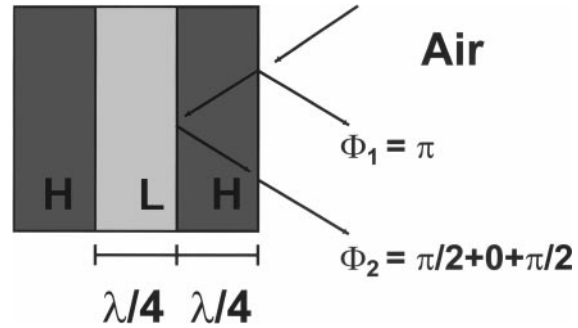


Fig. 2. Dispersion of dielectric high reflectors: operation of a quarterwave stack

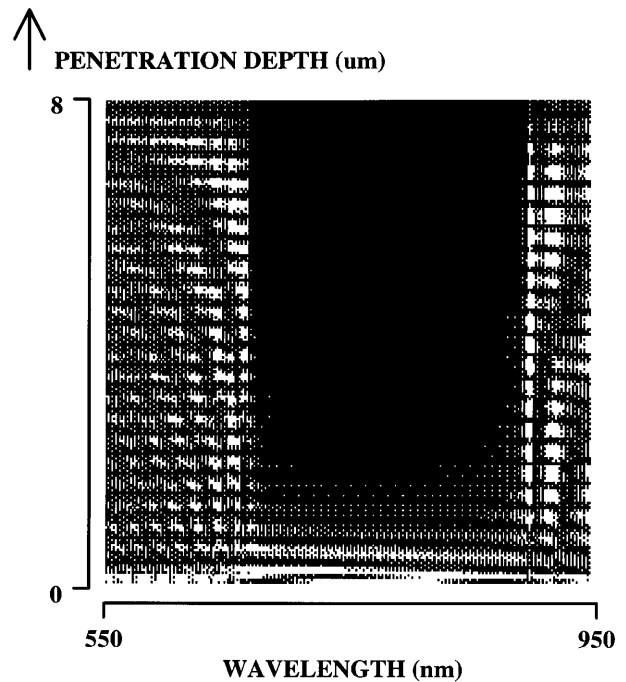


Fig. 3. Computed standing-wave electric field distribution in a quarterwave stack comprising $\text{TiO}_2/\text{SiO}_2$ layers with $\lambda/4$ optical thicknesses at 800 nm

accordance with the increased phase difference between the partial reflections. The lower the reflectivity the higher the penetration depth [17] of the electric field into the coating (see Fig. 3), which causes a frequency-dependent group-delay on reflection (see Fig. 4). The shape of the group delay vs. wavelength function exactly follows that of the standing wave electric field distribution in the multilayer stack [17], indicating that the group delay is ultimately determined by the penetration depth in this particular case [17]. It might be worth pointing out that quarterwave stacks exhibit a positive TOD at the reference wavelength, that can be used for (usually partial) compensation of the negative TOD of prism-pair-controlled laser oscillators.

The second effect that we refer to as *resonance* can be studied in its simplest form in a thin film realization of a Gires–Tournois interferometer (GTI) [18]. The general structure of GTI is shown in Fig. 5. It consists of an (ideal) $R = 100\%$ high reflector, a resonant cavity – which is similar to that of a Fabry–Pérot filter – and a top reflector, the reflectivity of which is set for the application problem. A thin

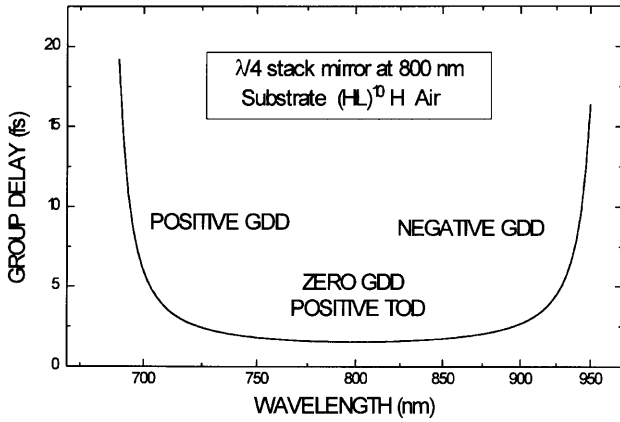


Fig. 4. Group delay vs. wavelength function of a quarterwave mirror corresponding to Fig. 3

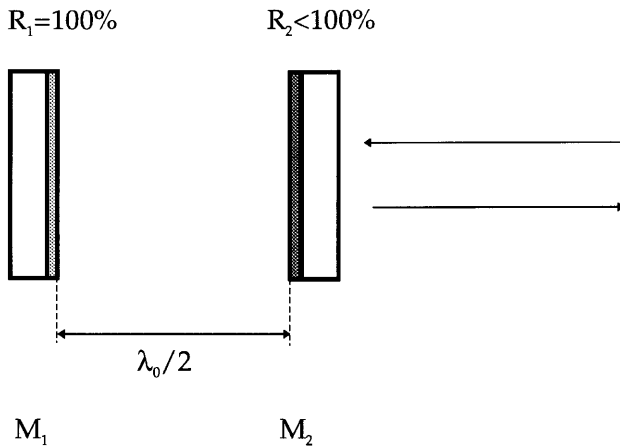


Fig. 5. Dispersion of dielectric high reflectors: a Gires–Tournois interferometer

film realization of such a (highly dispersive) high reflector might have the structure of Substrate | (HL)¹⁰ H 2L H | Air, where H and L correspond to $\lambda/4$ layers of high (H) and low (L) index dielectric materials. The computed group delay vs. wavelength function of such a thin film GTI is plotted in Fig. 6. At resonance, a GTI introduces the highest group delay – when the electric field is localized in the resonant cavity. At shorter wavelengths, a GTI shows a negative (anomalous) dispersion, whereas at longer wavelengths its group delay vs. wavelength function exhibits an opposite slope, i.e. normal dispersion. Initially, thin film GTIs were successfully applied for dispersion control in mode-locked dye lasers [19]. Later mirror-dispersion-controlled (MDC) fs pulse, mode-locked solid-state lasers were built this way [20], however, the pulse durations of these lasers were limited at around 40–50 fs according to the limited negative dispersion bandwidth of thin film GTIs [20].

Based on the Fourier theorem of dielectric multilayer devices [1, 21], *chirped dielectric laser mirrors* of gradient [21] or discrete index-valued [22] refractive index profiles were constructed in 1993, and were successfully implemented for intracavity broadband feedback and dispersion control in fs-pulse mode-locked solid-state lasers [1, 2, 13, 14]. Since then, they were adapted for different fs-pulse solid-state laser oscillators or parametric oscillators [1], for white-light continuum

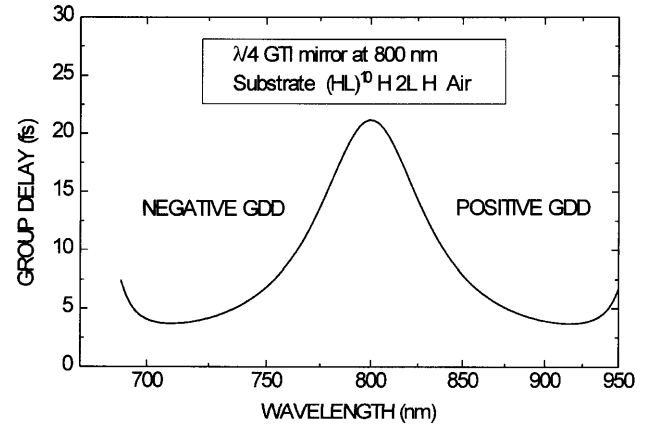


Fig. 6. Group delay vs. wavelength function of a Gires–Tournois interferometer

compression experiments [3] or fs-pulse optical parametric amplifiers [4], resulting in sub-5-fs optical pulses [3, 4]. From the theoretical point of view it is worth pointing out that the operation of chirped mirrors is based on the frequency-dependent penetration depth of the electric field [1, 22]: the different frequency components are reflected at different effective depths corresponding to the (chirped) Bragg wavelength along the plurality of layers. The *maximum group delay difference* over the high reflectivity range of the chirped mirror was found to be:

$$\Delta\tau_{\max} = \frac{2(t_{\text{chirped}} - t_{\text{qw}})}{c}, \quad (2)$$

where t_{chirped} is the optical thickness of the chirped mirror and t_{qw} is that of a standard quarterwave high reflector [22]. It is worth pointing out that – on the contrary – a higher group delay difference could be achieved in our novel multi-cavity Gires–Tournois mirrors that will be demonstrated in Sect. 3.

2 Frequency domain synthesis of chirped mirrors for sub-5-fs pulses [6]

Recently, we have discussed a few possibilities for obtaining initial designs for UBCMs with prescribed phase properties [1, 21]. Using the Fourier-transform technique reported in [1, 21, 23], UBCMs with negative second-order (GDD) and superimposed negative third-order dispersion were developed for the white-light continuum compression experiment reported in [3]. These mirrors exhibited high reflectivity (HR) from 580 to 1200 nm, i.e. over 267 THz [23]. By the exclusive use of four such mirrors, 6-fs pulses were obtained in the same experiment [1, 23]. In spite of the fact that the spectrum supported sub-4-fs pulses [3], fluctuation in the group delay vs. frequency function did not allow us to reach this theoretical value.

Since the invention of chirped mirrors [21, 22] several techniques have been developed for the construction of these optical thin-film devices [22] including direct computer optimization for the layer thicknesses of an initial, spatially chirped design [1, 2, 22], analytical approaches based on the Fourier-transform properties of optical interference coatings and on coupled-wave theory [1, 21, 24], along with semi-analytical approaches based on discrete layer thickness mod-

ulation for spacing multiple stopbands [25–27]. After the first reports on our current work [4, 6], an analytical approach for designing chirped mirrors with prescribed dispersion was also published by Matuschek et al. [28]. It is really a good thing that nowadays there are several alternative approaches and techniques for designing chirped mirrors with similar performances for different application requirements [1, 6, 27–29].

In this section we present a novel design approach [6] to obtain an initial design for realizing UBCMs with broad reflection bands and basically linear group delay vs. frequency functions. The dielectric layer structure is described in the spatial frequency domain rather than by the individual layer refractive indices and optical thicknesses, thus the optimization is performed only for a few parameters (6–8) instead of 40–60 parameters corresponding to the plurality of layers typically comprised in a chirped mirror design. We note that this spatial frequency domain description can be understood on the basis of our initial theoretical work [21] dealing with Fourier synthesis of mirrors with prescribed dispersive properties. In connection with our novel design approach, we must also refer to the recent works of Dods and Ogura [30], who used inverse spectral theory for designing dispersive mirrors.

It is known [21] that the logarithmic refractive index modulation corresponding to different Bragg frequencies must be set inversely proportional to the frequency in order to obtain a uniform reflectivity over the HR range of the mirrors. In practice, however, it is rather difficult to fabricate such a design due to problems with the available optical materials and thickness control inaccuracies [1]. However, the same behavior can be achieved in quarterwave stacks by detuning the relative optical thicknesses of the low (L) and high (H) refractive index layers, while keeping the Bragg period constant [24]: $OT_L + OT_H = \Lambda/2$, where OT_L and OT_H stand for the optical thickness values of the low- and high-index layers, respectively, and Λ is the Bragg wavelength.

In connection with chirped mirrors [1, 2, 6, 21–24, 27–29], the term ‘chirping’ means that we change the Bragg wavelength along the plurality of layers, hence the different frequency components are reflected at different effective depths called penetration depths [17]. Simple linear spatial chirping of the Bragg wavelength and a linear spatial detuning called ‘double chirping’ [24] does not automatically result in a linear group delay vs. frequency function. Furthermore, we usually have more general requirements for dispersive properties of chirped mirrors including prescribed values for second-, third-, and fourth-order dispersion as well. It is rather time consuming to use an analytical approach for obtaining an initial design [28], let us just mention the frequency-dependent refractive indices (dispersion) of the different layer materials. An additional problem is the reflectivity of the mirrors/air interface which requires additional impedance matching layers and a final computer refinement process [1, 24].

We came to the conclusion that the most straightforward way to obtain an (initial) design is to describe the chirped mirror structure in the spatial frequency domain expecting that change of the local Bragg-wavelength (Λ_i) and local detuning (α_i) of the i -th layer is a smooth function of i , hence it can be well approached by Taylor-series coefficients up to the

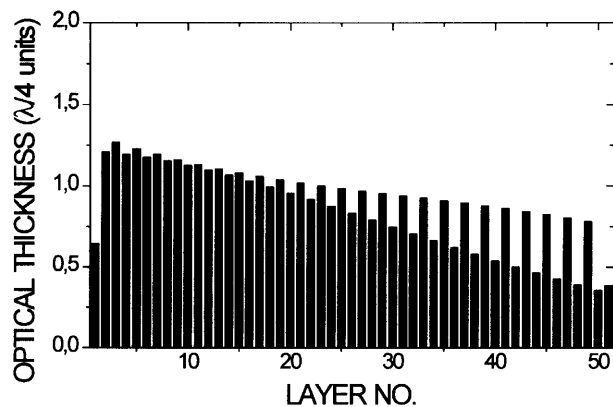


Fig. 7. Optical layer thickness coefficients of an ultrabroadband chirped mirrors design obtained by frequency domain optimization. Even and odd layers stand for TiO_2 and SiO_2 layers, respectively

third-order:

$$\Lambda_i = c_0 + c_1\beta_i + c_2(\beta_i)^2 + c_3(\beta_i)^3, \quad (3)$$

$$\alpha_i = d_0 + d_1\beta_i + d_2(\beta_i)^2 + d_3(\beta_i)^3. \quad (4)$$

In (3), $\beta_i = (i - n/2)/n$, where n stands for the number of unit periods ($i = 1..n$), and the i -th period is described as:

$$0.25\alpha_i\Lambda_iL \quad 0.5(1 - \alpha_i)\Lambda_iH \quad 0.25\alpha_i\Lambda_iL. \quad (5)$$

Given the specification on the second-, third-, and fourth-order dispersion for our UBCMs, we perform our optimization process for the c and d coefficients only (6–8 parameters), which results in an optimum solution within 1–2 minutes on a 266 MHz Pentium computer. Since the initial design is very close to the optimum solution, the final refinement process usually also takes another 1 to 5 minutes.

Recently we used the above-described algorithm for constructing chirped mirrors for the pulse-front-matched optical parametric amplifier described in [31]. We had the requirement for second- and third-order dispersion $D_2 = -173 \text{ fs}^2$, and $D_3 = -110 \text{ fs}^3$, respectively, over the wavelength range of 550 to 750 nm. In order to get a physically feasible solution, these values were divided by 5 (5 reflections on mirrors) for our specification. We chose our reference wavelength $\lambda = 640 \text{ nm}$ which corresponded to coefficient c_0 , and obtained the design shown in Fig. 7.

In Fig. 8, the computed group delay vs. frequency function is shown after the final optimization process together with measured values. Dispersion measurements were done for a pair of UBCMs with slightly shifted reference wavelengths for obtaining lower fluctuation in GDD [1]. The measured GDD of the mirror pair is in the $-35 - (-55 \text{ fs}^2)$ range between 560 nm and 710 nm.

The mirror pair presented was used for dispersion control in the experiment reported in [4] and resulted in 4.7-fs or tunable 7-fs pulses in the visible spectrum.

3 Multi-cavity Gires–Tournois interferometers as negative dispersion mirrors [7]

The increased bandwidth ($\approx 150 \text{ THz}$) of current chirped mirrors [1, 2, 6, 21–24, 27–29] relative to standard, quarterwave

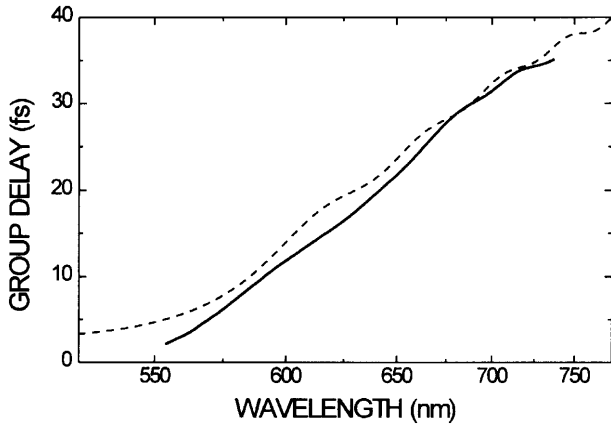


Fig. 8. Computed (dashed) and measured (continuous line) GDD of the ultrabroadband chirped mirror design after the final optimization and evaporation process. The design provides high reflectivity and a linear group delay versus frequency function over 145 THz

dielectric high reflectors (≈ 80 THz) was achieved at the expense of reduced reflectivities ($R \leq 99.8\%$) [1, 24, 27]. This fact directly follows from the Parseval theorem of optical interference coatings [21]:

$$\int_{-\infty}^{\infty} \left(\frac{n'(x)}{n(x)} \right)^2 dx = \int_{-\infty}^{\infty} |r(k)|^2 dk, \quad (6)$$

where $R(k) = |r(k)|^2$ is the intensity reflectivity at wavenumber k , ($k = \omega/c$), and $n'(x)/n(x)$ is the logarithmic derivative of the refractive index responsible for partial Fresnel reflections along the optical distance x . Obviously, given the technological constraint on the refractive index modulation and the overall optical thickness of a dielectric high reflector, the bandwidth of any high reflector can be increased only at the expense of reduced reflectivity.

A number of practical laser systems, however, require minimum reflection losses and high-order dispersion-free group-delay control over a frequency range of 50–80 THz, that still support (i) clear, pedestal-free, sub-15-fs pulses, or (ii) sub-100-fs pulses tunable over 100–120 nm around 800 nm. Such applications might well include; (a) sub-15-fs pulse generation in compact, mirror-dispersion-controlled, diode-pumped, fs pulse Cr:LiSAF and Cr:LiSGaF lasers [20, 32]; (b) low-pump-threshold, mirror-dispersion-controlled fs pulse Cr:LiSAF [33] or Ti:sapphire [14] lasers; or (c) highly efficient second-harmonic generation of tunable Ti:sapphire lasers in dispersion-compensated, mirror-dispersion-controlled laser cavities for the ultraviolet [34].

So far, two major types of dispersive mirrors have been tested in fs pulse laser systems: (i) thin-film Gires–Tournois interferometers (GTI) [19, 20] and (ii) chirped dielectric mirrors (CM) [1, 2, 13, 22, 24]. As we discussed in Sect. 1, there is a very important difference in the physical origin of their frequency-dependent group delay, however: in GTIs, the electric field is captured in Fabry–Pérot-like, resonant $\lambda/2$ cavities, whereas in CMs the group delay is strongly connected with the frequency-dependent penetration depth of the electric field. Hence (single-cavity) GTIs suffered from higher-order dispersion limiting the laser performance to

40–50 fs pulses [20], whereas CMs currently allow generation of pulses with durations less than 5 fs [3, 4].

During our recent studies we found that there is an alternative approach for obtaining *pure quadratic phase shift on reflection* from such dielectric mirrors: it can be realized with multi-cavity GTIs (MCGTIs) as well. The initial design was obtained by the needle optimization technique [35, 36] using a special, upgraded version of our “Optilayer” software. After a final refinement process we came to the solution shown in Fig. 9. In conventional (single-cavity) thin film GTIs, the layer structure consists of $\lambda/4$ stack with a single $\lambda/2$ resonant cavity layer on the top of the quarterwave mirror [19, 20]. In this novel design [7] more than one (in this example three) separate slightly detuned $\lambda/2$ cavities (layer 26, 30, and 34) with embedded $\lambda/4$ layers are responsible for the dispersive properties of the mirror. The computed GDD vs. wavelength function of the design is shown in Fig. 10. The central wavelength of the design was chosen to be $\lambda = 0.8 \mu\text{m}$ in this specific case. The design provided a negative GDD of $-50 \pm 1 \text{ fs}^2$ over a bandwidth of 56 THz. For comparative purposes, the computed GDD of a single-cavity GTI is also plotted in the figure. The *quarterwave layer mirror stack* (layers 1 to 25) provided the extremely high reflectivity of the design that is shown in Fig. 11.

It is worth pointing out that the GDD function and the reflectivity shown in Figs. 10 and 11 (plotted with continuous lines) can be fabricated with the use of state-of-the-art coating deposition technologies, such as ion-beam sputtering [37]. Another important issue is that the layer structure can be easily adapted for any other wavelength regime from the ultra-violet to the near infrared simply by rescaling the layer thicknesses. Our recent laser experiments [34] show that our multi-cavity GTIs show negligible reflection losses even in the ultraviolet; the standing electric field is concentrated in the SiO₂ layers which have relatively low absorption and scattering losses.

Before we show our experimental results, the following question should be addressed: is there a proof of that dispersion of MCGTIs originates from resonances rather than the frequency-dependent penetration depth (as in case of negative dispersion mirrors referred to as chirped mirrors)? Our answer is yes. In Fig. 12, computed group delay vs. wavelength

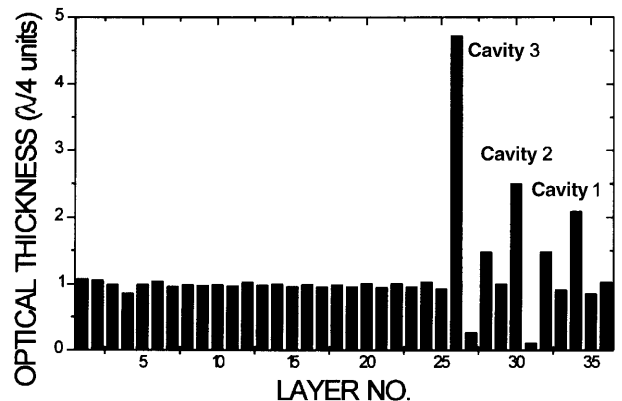


Fig. 9. Optical layer thickness coefficients of a multi-cavity thin-film Gires–Tournois interferometer. The design provides high-order dispersion-free negative GDD over a bandwidth of 56 THz with theoretical reflectivities higher than 99.97%. Even and odd layers stand for SiO₂ and TiO₂ layers, respectively

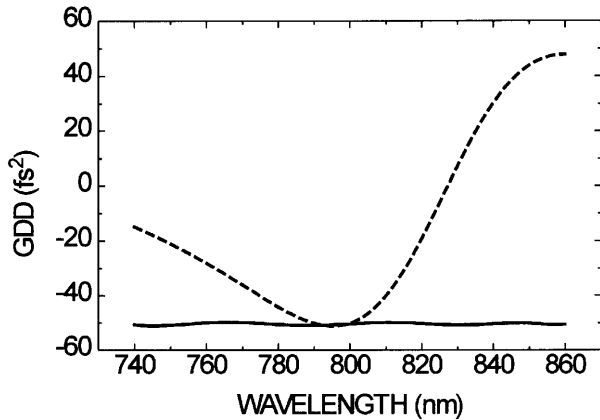


Fig. 10. Computed GDD of the multi-cavity GTI (continuous line) compared to that of a conventional single-cavity GTI (dashed)

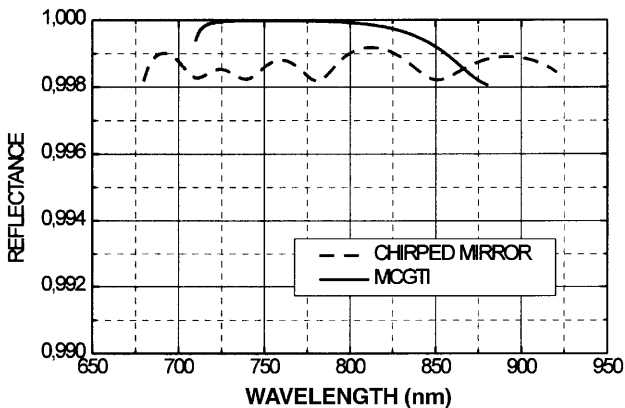


Fig. 11. Computed reflectance of the multi-cavity GTI (continuous line) compared to that of a standard chirped mirror design (dashed)

function of a MCGTI with an increased GDD is shown. During the design, the overall optical thickness and number of layers forming the quarterwave stack were kept constant, only optical thicknesses of the top layers were varied. From the calculation of the overall optical thickness of the top (phase correction) layers, the maximum group delay difference that could have been obtained over the high-reflectivity range (see (2)) was limited to 36 fs – if it is connected with the frequency-dependent penetration depth only. However, the computed difference is definitely higher: it reaches values up to 40–45 fs.

Additionally, we have studied distribution of the standing-wave electric field in the MCGTI design shown in Fig. 9: we found that the electric field is mostly localized in the (coupled) cavities shown in Fig. 9, whereas it has relatively low intensities in the impedance matching layers between them. We found that the electric field is captured by one or two of the cavities at each wavelength. By tuning the wavelength, the electric field is shifting gradually from one cavity to the next one. Finally, the change of electric field in the layer structure results in a linear group delay vs. wavelength function according to the “localization” of the electric field. During the optimization process, the “strength” and length of the cavities are adjusted by the layer thicknesses. Experiments are in progress for utilizing the features of our novel design in different fs-pulse laser systems de-

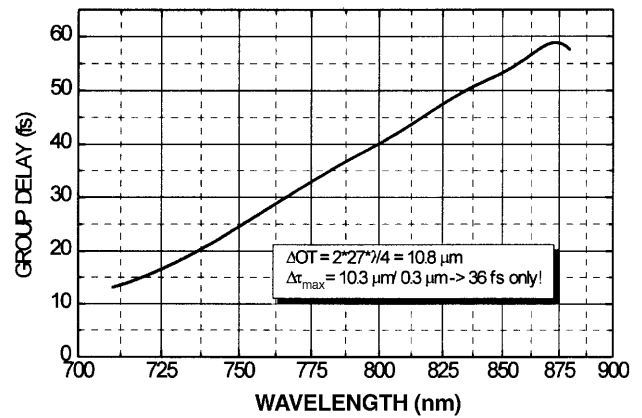


Fig. 12. Computed group delay vs. wavelength function of a multi-cavity GTI designed for higher values of GDD

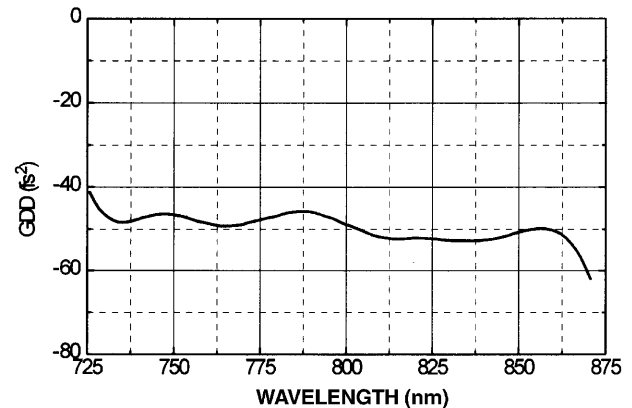


Fig. 13. Measured GDD of an ion-beam sputtered multi-cavity GTI designed for full dispersion control in a tunable sub-100-fs Ti:S laser oscillator

scribed above [8, 13, 32–34]. As an example, measured GDD vs. wavelength function of a MCGTI designed for a mirror-dispersion-controlled, sub-100-fs, tunable Ti:S laser is plotted in Fig. 13 (the measured GDD function corresponds to the theoretical curve previously shown in Fig. 10). Based on our experimental results, we are convinced that multi-cavity GTI mirrors will find their applications similarly to chirped laser mirrors owing to their simple structure (hence relatively low manufacturing costs), high reproducibility and extremely low reflection losses ($R > 99.95\%$). Among others, we found that MCGTIs are promising candidates for constructing high-efficiency MDC Ti:sapphire lasers comprising relatively long (optical path ≥ 4 mm) Ti:sapphire crystals with sub-15-fs performance, and for constructing MDC tunable oscillators with sub-100-fs performance over a bandwidth of 50–60 THz.

4 Conclusion

In this paper, we presented a novel design technique referred to as frequency domain synthesis of chirped mirrors. These mirrors exhibit high reflectivity and nearly constant group delay over 150 THz supporting generation of sub-5-fs pulses in the visible. Later, multi-cavity thin-film Gires–Tournois interferometers were introduced as an alternative approach to

realize “negative dispersion mirrors”. These novel dielectric high reflectors exhibit reflectivities $R > 99.97\%$ and a negative group delay dispersion of $-50 \pm 1 \text{ fs}^2$ over a bandwidth of 56 THz.

Acknowledgements. This research was partially supported by the OTKA Science Foundation of Hungary under grants T 029578 and T 022563, the Bolyai Scholarship of the Hungarian Academy of Sciences, and by companies of MLD Technologies and R&D Lézer-Optika Bt.

References

- R. Szipöcs, A. Köházi-Kis: Appl. Phys. B **65**, 115 (1997)
- E.J. Mayer, J. Möbius, A. Euteneuer, W.W. Rühle, R. Szipöcs: Opt. Lett. **22**, 528 (1997)
- A. Baltuska, Z. Wei, M.S. Pshenichnikov, D.A. Wiersma, R. Szipöcs: Appl. Phys. B **65**, 175 (1997)
- A. Shirakawa, I. Sakane, T. Kobayashi: *Ultrafast Phenomena XI* (Springer, Berlin, Heidelberg 1998) p. 54
- J.K. Ranka, R.S. Windeler, A.J. Stentz: Opt. Lett. **25**, 25 (2000)
- R. Szipöcs: Technical Digest of Ultrafast Optics 99 conference, Monte Verita, Ascona, Switzerland, July 11–16, 1999 pp. 130–133
- R. Szipöcs, G. DeBell, A.V. Tikhonravov, M.K. Trubetskov: Ibid. pp. 70–73 (1999)
- A. Köházi-Kis, P. Apai, S. Lakó, R. Szipöcs: Ibid. pp. 66–69 (1999)
- R. Szipöcs, A. Köházi-Kis, P. Apai, E. Finger, A. Euteneuer, M. Hofmann: Ibid. pp. 74–77 (1999)
- F. Abeles: Ann. Phys. **12**(5), 596–640, 706–784 (1950)
- H.A. Macleod: Basic theory, Chapt. 2, In *Thin Film Optical Filters* (Adam Hilger, Bristol 1985)
- C. Spielmann, R. Szipöcs, A. Stingl, F. Krausz: Phys. Rev. Lett. **73**, 2308 (1994)
- L. Xu, C. Spielmann, F. Krausz, R. Szipöcs: Opt. Lett. **21**, 1259 (1996)
- R. Szipöcs, F. Krausz: US Pat. No. 5,734,503 (1998)
- R. Szipöcs, E. Finger, A. Euteneuer, M. Hofmann, A. Köházi-Kis: Laser Phys. Vol. 10, No.2 (in press) (2000)
- A.V. Tikhonravov, P.W. Baumeister, K.V. Popov: Appl. Opt. **36**, 4382 (1997)
- D.I. Babić, S.W. Corzine: IEEE J. Quantum Electron. **QE-28**, 514 (1992)
- F. Gires, P. Tournois: C. R. Acad. Sci. **258**, 6112 (1964)
- J. Heppner, J. Kuhl: Appl. Phys. Lett. **47**, 453 (1985)
- I.T. Sorokina, E. Sorokin, E. Wintner, A. Cassanho, H.P. Janssen, R. Szipöcs: Opt. Lett. **21**, 1165 (1996)
- R. Szipöcs, A. Köházi-Kis: Proc. Soc. Photo-Opt. Instrum. Eng. **2253**, 140 (1994)
- R. Szipöcs, K. Ferencz, C. Spielmann, F. Krausz: Opt. Lett. **19**, 201 (1994)
- A. Köházi-Kis, R. Szipöcs: In Technical Digest of Novel Lasers, Devices and Application Topical Meeting, Munich, June 18–19, 1997
- F.X. Kartner, N. Matuschek, T. Schibli, U. Keller, H. Haus, C. Heine, R. Morf, V. Scheuer, M. Tilsch, T. Tschudi: Opt. Lett. **22**, 831 (1997)
- B.E. Perrilloux: OSA 1998 Technical Digest Series **9**, 319 (1998)
- B.E. Perrilloux: Appl. Opt. **37**, 3527 (1998)
- G. Tempea, F. Krausz, C. Spielmann, K. Ferencz: IEEE J. Top. Quantum Electron. **4**, 193 (1998)
- N. Matuschek, F. Kartner, U. Keller: IEEE J. Quantum Electron. **QE-35**, 129 (1999)
- V. Laude, P. Tournois: CLEO 1999, paper CTuR4, Baltimore, USA (1999)
- S.R.A. Dods, M. Ogura: Appl. Opt. **36**, 7741 (1997)
- A. Shirakawa, I. Sakane, T. Kobayashi: Opt. Lett. **23**, 1292 (1998)
- I.T. Sorokina, E. Sorokin, E. Wintner, A. Cassanho, H.P. Janssen, R. Szipöcs: Opt. Lett. **22**, 1716 (1997)
- G.J. Valentine, J.M. Hopkins, P. Loza-Alvarez, G.T. Kennedy, W. Sibbett, D. Burns, A. Valster: Opt. Lett. **22**, 1639 (1997)
- S. Lakó, P. Apai, R. Szipöcs: Highly efficient second-harmonic-generation in mirror-dispersion controlled ring cavities for the ultraviolet, CLEO/Europe, Paper CThE13 2000
- A.V. Tikhonravov, M.K. Trubetskov: Proc. Soc. Photo-Opt. Instrum. Eng. **2253**, 10 (1994)
- A.V. Tikhonravov, M.K. Trubetskov, A.A. Tikhonravov: OSA 1998 Technical Digest Series **9**, 293 (1998)
- G. DeBell, L. Mott, M. von Gunten: Proc. Soc. Photo-Opt. Instrum. Eng. **895**, 254 (1988)